Carbon Electrode–Molecule Junctions: A Reliable Platform for Molecular Electronics

Chuancheng Jia,[†,§] Bangjun Ma,[†,§] Na Xin,[†] and Xuefeng Guo*[,†,‡]

[†]Center for Nanochemistry, Beijing National Laboratory for Molecular Sciences, State Key Laboratory for Structural Chemistry of Unstable and Stable Species, College of Chemistry and Molecular Engineering, Peking University, Beijing 100871, P. R. China

[‡]Department of Materials Science and Engineering, College of Engineering, Peking University, Beijing 100871, P. R. China

CONSPECTUS: The development of reliable approaches to integrate individual or a small collection of molecules into electrical nanocircuits, often termed "molecular electronics", is currently a research focus because it can not only overcome the increasing difficulties and fundamental limitations of miniaturization of current silicon-based electronic devices, but can also enable us to probe and understand the intrinsic properties of materials at the atomic- and/or molecular-length scale. This development might also lead to direct observation of novel effects and fundamental discovery of physical phenomena that are not accessible by traditional materials or approaches. Therefore, researchers from a variety of backgrounds have been devoting great effort to this objective, which has started to move beyond simple descriptions of charge transport and branch out in different directions, reflecting the interdisciplinarity. This Account exemplifies our ongoing interest and great effort in developing efficient lithographic methodologies capable of creating molecular electronic devices through the combination of top-down micro/nanofabrication with bottom-up molecular assembly. These devices use nanogapped carbon nanomaterials (such as single-walled carbon nanotubes (SWCNTs) and graphene), with a particular focus on graphene, as point contacts formed by electron beam lithography and precise oxygen plasma etching. Through robust amide linkages, functional molecular bridges terminated with diamine moieties are covalently wired into the carboxylic acid-functionalized nanogaps to form stable carbon electrode–molecule junctions with desired functionalities.
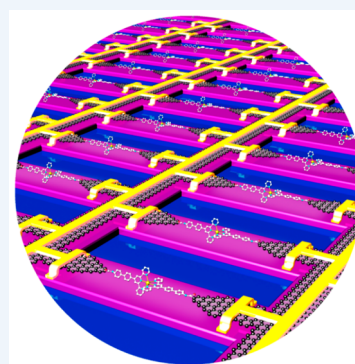
At the macroscopic level, to improve the contact interface between electrodes and organic semiconductors and lower Schottky barriers, we used SWCNTs and graphene as efficient electrodes to explore the intrinsic properties of organic thin films, and then build functional high-performance organic nanotransistors with ultrahigh responsivities. At the molecular level, to form robust covalent bonds between electrodes and molecules and improve device stability, we developed a reliable system to immobilize individual molecules within a nanoscale gap of either SWCNTs or graphene through covalent amide bond formation, thus affording two classes of carbon electrode–molecule single-molecule junctions. One unique feature of these devices is the fact that they contain only one or two molecules as conductive elements, thus forming the basis for building new classes of chemo/biosensors with ultrahigh sensitivity. We have used these approaches to reveal the dependence of the charge transport of individual metallo-DNA duplexes on π-stacking integrity, and fabricate molecular devices capable of realizing label-free, real-time electrical detection of biological interactions at the single-event level, or switching their molecular conductance upon exposure to external stimuli, such as ion, pH, and light.

These investigations highlight the unique advantages and importance of these universal methodologies to produce functional carbon electrode–molecule junctions in current and future researches toward the development of practical molecular devices, thus offering a reliable platform for molecular electronics and the promise of a new generation of multifunctional integrated circuits and sensors.

1. INTRODUCTION

Optoelectronic devices are the basis of modern informational world, so there is a continuous impetus to decrease their size, enhance their performance and increase their variety of functions.[1,2] However, in accordance with Moore's law, the top-down fabrication techniques developed for conventional silicon-based electronics have nearly reached their miniaturization limitation, implying that an intrinsic change is necessary to produce a new generation of intelligent devices with smaller dimensions and superior performances. Due to the ultrasmall dimensions, abundant diversity, and designable functions of

molecules, the creation of optoelectronic devices using individual or a small collection of molecules as core components, so-called "molecular electronics", is a promising bottom-up approach to breakthrough the development bottleneck of current microelectronics.[3−9]

In fact, this concept of building optoelectronic devices based on the properties inherent in individual molecules has led to remarkable technological and theoretical developments in the

past decades.[4,9−22] There have been a number of discrete approaches developed for molecular transport junction fabrication, including break junctions, scanning probe techniques, sandwich electrodes, lithographic methods, mercury drop electrodes, and others (refs 23−25 and references therein). These substantial progresses undoubtedly lay the foundation for both measurement capabilities and fundamental understanding of various physical phenomena of these conceptually simple molecular transport junctions—consisting of only one or a few molecules—that are beyond conventional electronic transport properties, such as electromechanics, thermoelectronics, quantum interference, optoelectronics, and spintronics. Despite these considerable achievements, there are still no commercially available molecular electronics. To satisfy requirements for real applications, the development of practical molecular devices with high stability and specific functions is the prerequisite. This is extremely challenging because it necessitates easy fabrication and precise control of reliable devices, which depend on several factors including the testbed architectures used, the number and defect density of molecules being tested, and the nature of the molecule/electrode interface.[5,26]

Among various platforms of molecular transport junctions, carbon electrode−molecule junctions,[11,27] where carbon nanomaterials such as single-walled carbon nanotubes (SWCNTs) and graphene are used as nanoscale electrodes, are particularly attractive because of their unique advantages. Both SWCNTs and graphene are low-dimensional carbon nanomaterials made entirely of sp^2-hybridized carbon atoms arranged in a honeycomb lattice, offering a natural compatibility with organic/biological molecules. In addition, they exhibit extraordinary electronic properties along with easy processability. Unlike mobile metal electrodes, they are atomically stiff, infinitely large, and naturally functional at their ends. When lithographically patterned as point contacts, they are end-functionalized by carboxylic acid groups. These functional groups are used to form robust covalent bonds at the molecule/electrode interface through amide linkages that can endure chemical treatments and external stimuli, thus markedly improving device stability. Another important feature of these point contacts is that they are molecular in size, ensuring the number of bridged molecules down to the single-molecule level. Compared with one-dimensional SWCNTs, graphene is a two-dimensional crystalline monolayer, and it enables the facile fabrication of point contact arrays. This largely simplifies the device fabrication process and affords stable molecular devices in high yield. As a result of all of these features, SWCNTs and, in particular, graphene are ideal complementary contacts to test the intrinsic properties of various molecular devices with molecular sizes in all dimensions. These techniques hold great promise to realize functional molecular devices that can convert molecular functions into detectable electrical signals with ultrahigh sensitivity, thus rendering carbon electrode−molecule junctions as a reliable platform for molecular electronics toward practical applications. In this Account, we detail the methodologies used to develop such a molecular electronics platform, the sensing applications of this platform, and the developing trends of this field.

2. GENERAL STRATEGIES TO MAKE NANOGAPPED CARBON POINT CONTACTS

2.1. Electron Beam Lithography to Make SWCNT Point Contacts

To form SWCNT point contacts, individual SWCNTs are sliced by electron beam lithography and selective oxygen plasma oxidative etching, leaving carboxylic-acid-capped ends with a gap size of less than 10 nm. Conductive molecules terminated by amines are then used to covalently bridge nanogapped SWCNT electrodes through amide linkages, forming the first class of carbon electrode−molecule single-molecule junctions: SWCNT electrode−molecule single-molecule junctions. This process has been well established for a reported system.[11] In this Account, we mainly aim to update the reader with recent progress in this field, including how to realize label-free, real-time electrical detection of biological interactions at the single-event level, which demonstrates a novel and invaluable direction for future single-molecule electrical biodetection.

2.2. Dash-Line Lithography to Form Graphene Point Contacts

Graphene is a two-dimensional zero-bandgap semimetal carbon material with extraordinary electronic properties that is widely used in nanoelectronics.[28] Compared with one-dimensional SWCNTs, graphene has homogeneous high electric conductivity and is more convenient for device processing and integration. Using graphene as point contacts, we developed the second class of carbon electrode−molecule single-molecule junction: graphene electrode−molecule single-molecule junctions.[27] Similar to the SWCNT system above, high-quality single-layer graphene sheets are first obtained on silicon substrates by either a chemical vapor deposition and subsequent transfer[29] or a peeling-off technique,[30] and spin-cast with a layer of poly(methyl methacrylate) (PMMA). Then, an array with holes of <10 nm is formed in the PMMA masking layer by applying a Design CAD file of a 5 nm width dashed line through electron beam lithography in a process called dashed-line lithography (DLL) (Figure 1A). The graphene sheet is then locally cut by oxygen plasma ion etching through the holes in the PMMA layer. By exploiting the gradual etching and undercutting of PMMA, we achieved nanogaps between indented graphene point contacts. This DLL technique is able to produce carboxylic acid terminated graphene point contact arrays with narrow gaps (Figure 1B). These point contacts react with molecule bridges derivatized with amino groups to form molecular devices in high yields.

3. FUNCTIONAL ORGANIC FIELD-EFFECT NANOTRANSISTORS

In general, the nature of the semiconductor/electrode interface that is ubiquitous in organic field-effect transistors (OFETs) plays a vital role in device performance and stability because charge injection and extraction occur at this interface under an applied electric field. Both SWCNTs and graphene are composed of carbon six-membered rings with a work function of about 4.5−5.0 eV, which is a good match with organic semiconductors. Therefore, high-quality physical contacts are expected to form between carbon electrodes and molecules at the macroscopic level, making them well-suited as carrier injection electrodes for OFETs.[16,31] In this section, we summarize recent systematic applications of graphene as
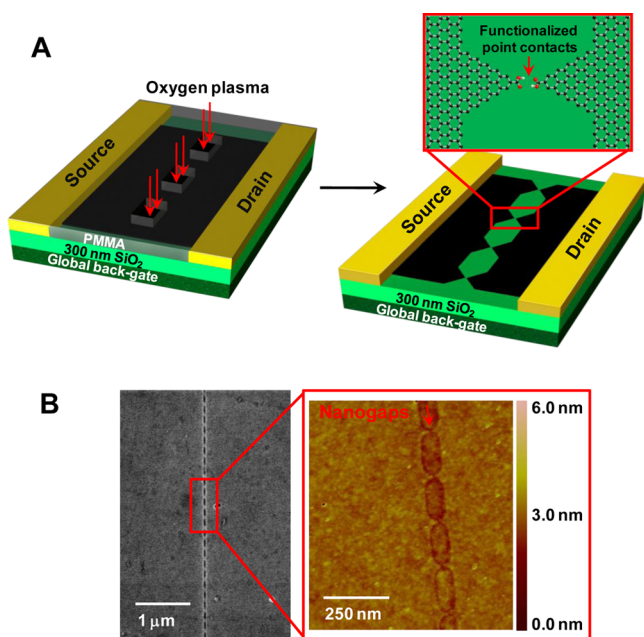
Figure 1. (A) Schematic representation of cutting graphene by DLL-defined oxygen plasma oxidative etching to form indented graphene point contact arrays that are capped with carboxylic acids. (B) SEM (left) and AFM (right) images of an indented graphene point contact array.

efficient electrodes to make stimuli-responsive, CMOS-compatible OFETs.

Using the same lithographic procedure as for SWCNTs above, two-dimensional pristine single-layer graphene sheets (with a work function of ~4.5−4.9 eV) obtained by a peeling-

off technique can be patterned as nanoscale planar source/drain electrodes (Figure 2A and B). For example, thin films of poly(3-hexylthiophene-2,5-diyl) (P3HT) from a diluted chloroform solution have been incorporated into nanoscale graphene electrodes to form planar graphene-P3HT transistors.[32] Because of the disordered molecular packing in P3HT thin films, the calculated carrier mobility (μ) and photoresponsivity were moderate at ~1.4×10^{-3} cm^2 V^{-1} s^{-1} and ~8.3 A W^{-1}, respectively. To improve the molecular organization and thus device performance, we used a Langmuir−Blodgett bottom-up approach to fabricate dense, well-ordered self-assembled monolayers of copper phthalocyanine (CuPc), a typical organic semiconductor with an ionization potential of 5.0−5.2 eV.[33] These monolayers were then positioned into the nanogap of planar graphene electrodes to form a new class of photoresponsive high-performance molecular field-effect transistors (inset of Figure 2C). These graphene-CuPc monolayer transistors showed bulklike carrier mobility of as high as 0.04 cm^2 V^{-1} s^{-1}, high on/off current ratios of over 10^6, and high reproducibility of almost 100%. This is significant, considering that the charge transport in the monolayer transistors occurs from a single 1.3 nm-thick monolayer. Another remarkable property of these devices is their ultrasensitivity to light. The best responsivity of these devices is very high at ~7.10×10^5 A W^{-1} (Figure 2D). This strong photoresponse might be caused by an integrated mechanism; for example, because of buildup of electron-trapped charges at the semiconductor/dielectric interface during illumination over tens of seconds.

To understand how the device architecture affects the light-responsive efficiency and further enhance the photoresponsivity of carbon electrode-based organic transistors, in our recent work, blends of P3HT and [6,6]-phenyl-C61-butyric acid methyl ester (PCBM) were used as photoresponsive semi-
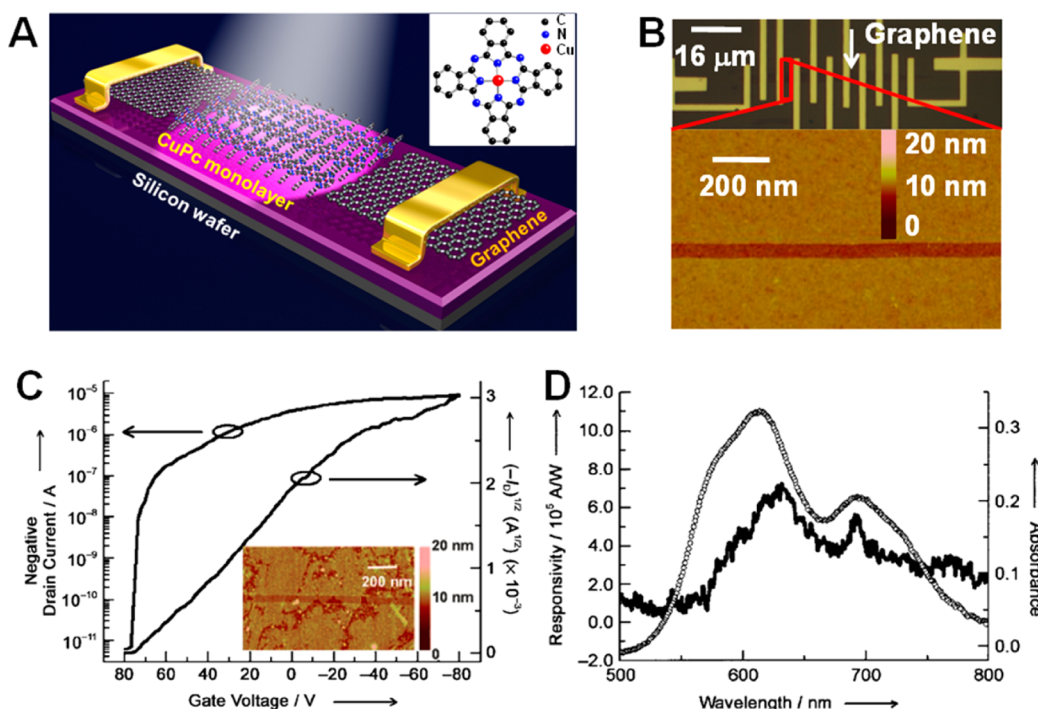

Figure 2. (A) Schematic illustration of a CuPc monolayer transistor with nanogapped planar graphene electrodes. (B) Optical micrograph and AFM image of planar graphene nanoelectrodes with a gap size of about 50 nm. (C) Transfer characteristics of the device. Inset: AFM image of the nanogapped graphene electrodes after CuPc monolayer assembly. $V_D = -15$ V. (D) Wavelength-dependent photoresponsive behavior of the device, which matches the UV/vis absorption spectrum of CuPc thin films.
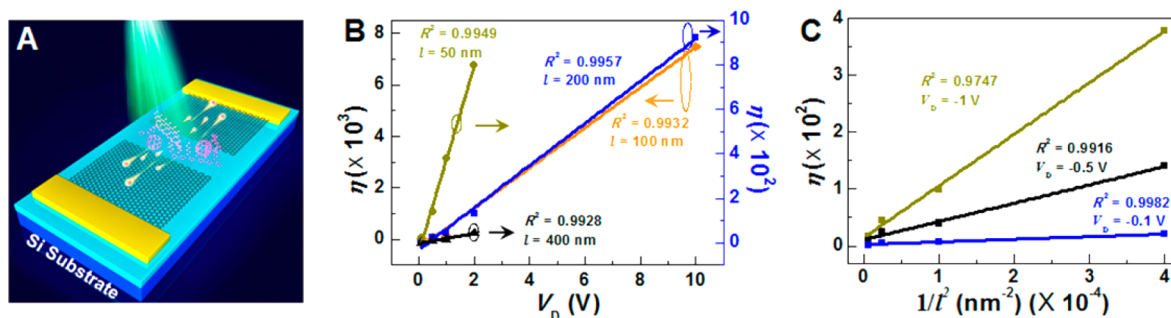
Figure 3. (A) Device structure of a graphene-based P3HT:PCBM hybrid photodetector. (B) Linear fits of photogains η and source-drain bias voltage V_D for gap lengths l of 50, 100, 200, and 400 nm (λ = 540 nm; V_G = 0 V). (C) Linear fits between η and the reciprocal of the square of l at V_D of −0.1, −0.5, and −1 V (λ = 540 nm; V_G = 0 V).
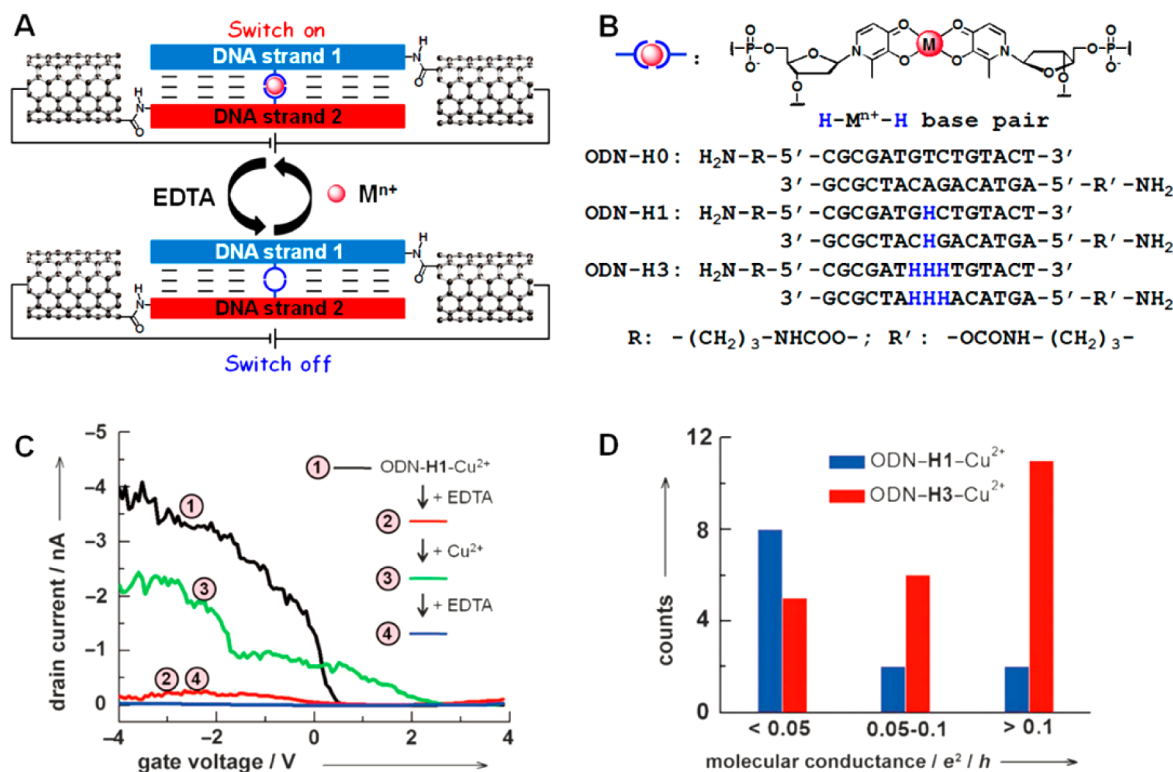

Figure 4. (A) Schematic representation of the sensing process of SWCNT−metallo-DNA junctions. (B) Molecular structure of a Cu^{2+}-mediated base pair and the DNA sequences used. (C) Electrical characteristics of an ODN−H1−Cu^{2+}-bridged device after different treatments. V_D = −50 mV. (D) Comparison between the conductance of ODN−H1−Cu^{2+} and ODN−H3−Cu^{2+}.

conductors to make ultrasensitive nanoscale hybrid photo-detectors with tunable channel lengths (Figure 3A).[34] Assuming that the transport of free carriers in the P3HT:PCBM layer is mainly controlled by a "hopping" mechanism, the photogain (η) in the active layer is strongly dependent on both the driving voltages (V_D) and hopping distance, that is, the distance between the source and the drain, or gap length (l). By systematically tuning the voltage biases and the gap sizes, we found that η is proportional to V_D (Figure 3B) and inversely proportional to the square of l (Figure 3C), respectively. This relation can be expressed by the following equation

$$\eta \propto \frac{V}{l^2} \tag{1}$$

This relationship is well explained by another gain factor (G),[35] defined by

$$G = \frac{\tau_c}{\tau_t} = \frac{\tau_c \mu V}{l^2} \tag{2}$$

where τ_c is the lifetime of the photogenerated carriers and τ_t is the time required for the carriers moving from one electrode to another, considering the fact that τ_c and μ are the intrinsic properties of the materials. Therefore, the unique device architecture, tunability of nanoscale channel lengths, and optimized contact nature of semiconductor/electrode interfaces led to ultrahigh η of over 10^3 when graphene was used as electrodes and over 10^6 when SWCNTs were used as electrodes. Such carbon electrode-based photodetectors may become a fundamental device platform for optical information, logic circuit and sensing applications.

4. CARBON ELECTRODE−MOLECULE SINGLE-MOLECULE JUNCTIONS

At the molecular level, individual molecules with amines on both ends are used to bridge carboxylated carbon electrodes to
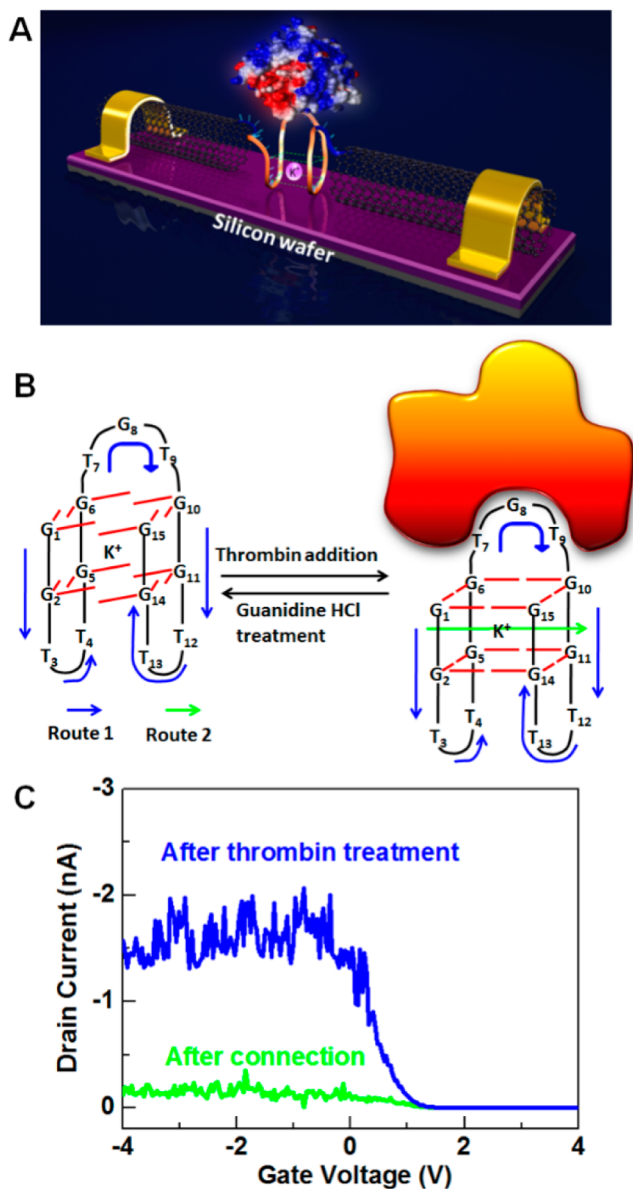

Figure 5. (A) Schematic representation of SWCNT−DNA aptamer junctions. (B) Sensing mechanism of protein binding to strengthen the π stacking of G4 conformation. (C) Electronic characteristics of the device after DNA aptamer connection and thrombin treatment. $V_D = -50$ mV.

form carbon electrode−molecule single-molecule junctions through robust covalent amide bonds.[11,27] This architecture substantially enhances device stability, which is of crucial importance for future practical applications. Another important attribute of these junctions is that they have only one or two molecules as molecular probes, thus setting the foundation for building new classes of ultrasensitive chemo/biosensors with the ultimate aim of detecting single-molecule events in natural samples. Here, we demonstrate the capability of installing molecular functions into electrical nanocircuits in the new platform of carbon electrode−molecule junctions.

4.1. SWCNT−Molecule Single-Molecule Junctions

4.1.1. Metallo-DNA Conductivity. Previous studies reported that pristine DNA has limited conductivity, which limits the potential of DNA-based nanoelectronics.[11] A promising solution to improve the conductivity of DNA is to replace some or even all the base pairs in DNA with metal complexes because synthesis of metallo-DNA is well established and programmable.[36] To prove this, we demonstrated the first direct electrical conductance measurements of individual metallo-DNA duplexes based on the SWCNT−molecule junctions (Figure 4A).[37] Three different DNA duplexes that were functionalized with amines at both ends were used to covalently bridge the carboxylic acid-capped gaps in the SWCNTs (Figure 4B), thus forming SWCNT−metallo-DNA junctions. A pair of bases in the middle of a 15 nucleotide duplex was replaced by hydroxypyridone nucleobases (H) to afford ODN-H1, which forms a stable complex in the presence of Cu^{2+}. Similarly, ODN-H3 contained three consecutive pairs of hydroxypyridone nucleobases in the middle of the duplex that replaced the corresponding pairs.

The conductance characteristics of a representative device containing ODN−H1-Cu^{2+} under different conditions are shown in Figure 4C. The source/drain current was partially recovered after ODN−H1-Cu^{2+} reconnected the open circuit with the conductance of 2.1×10^{-3} e^2/h. When the devices were annealed above the melting temperature of the DNA duplex in an EDTA buffer solution, the conductance decreased markedly to 1.0×10^{-4} e^2/h. This is because EDTA removed Cu^{2+} from the metallo-base pair and consequently broke the π-stacked charge transport path. Remarkably, device conductance increased dramatically upon subsequent treatment with Cu^{2+} (1.3×10^{-3} e^2/h) and then decreased again in EDTA buffer solution (1.0×10^{-4} e^2/h). The cyclic changes in device conductance upon alternate treatment with Cu^{2+} and EDTA occurred several times until the devices degraded because of unexpected interactions between species in the solutions and DNA. This reversible conductance switching was universal as demonstrated by alternate treatment with EDTA and other metals such as Ni^{2+} and Fe^{3+} instead of Cu^{2+}. Treatment of the devices with Fe^{3+} showed the best reversibility.

These results consistently prove that, compared with the case of mismatch-like metal-free DNA, the introduction of metal ions inside the DNA core strengthens the π-stacking between base pairs. This effect can facilitate charge transport in DNA, thus suggesting that it may be possible to improve DNA conductivity by increasing the number of metal ions. To prove this, we compared the conductance of ODN−H1-Cu^{2+} and ODN−H3−Cu^{2+} (Figure 4D). The conductance of ODN−H3-Cu^{2+} was much higher than that of ODN−H1−Cu^{2+}, despite the device-to-device variation of conductance. Therefore, we provided the first experimental support confirmation that the electrical conductance of natural DNA duplexes can be improved by rational arrangement of metal-mediated base pairs in DNA frameworks.

4.1.2. SWCNT−DNA Single-Molecule Biosensors. As proved by the above-mentioned experiments, a probe molecule integrated into single-molecule junctions provides the basis for ultrasensitive detection when it specifically binds to other chemical or biological molecules. Using a similar approach with SWCNTs as point contacts, we developed new SWCNT−DNA junctions by covalently connecting cut SWCNTs with a DNA aptamer (Figure 5A). These SWCNT−DNA aptamer junctions
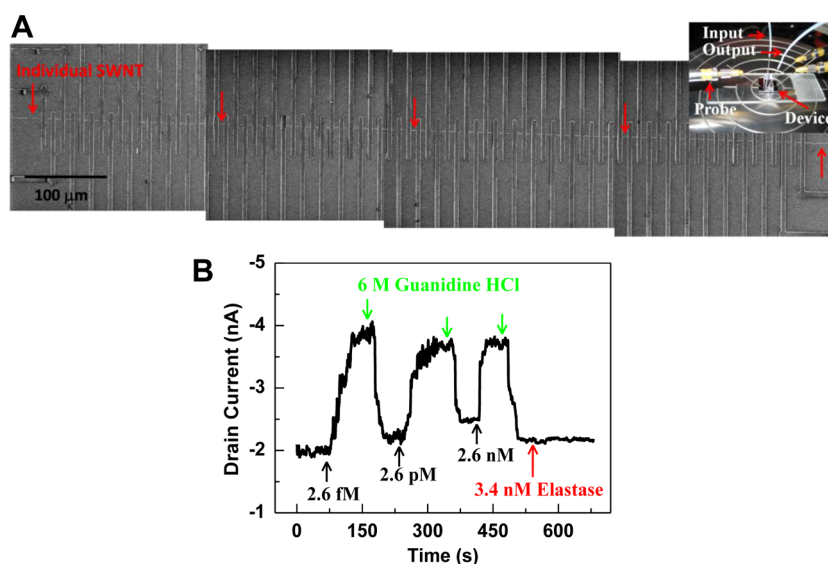
Figure 6. (A) SEM images of a highly integrated SWCNT array. Inset is an optical image of a device during real-time measurement. (B) Reversible conductance changes at different thrombin concentrations are essentially independent of concentration, demonstrating the reproducibility and single-molecule sensitivity. $V_D = -50$ mV, $V_G = 0$ V.
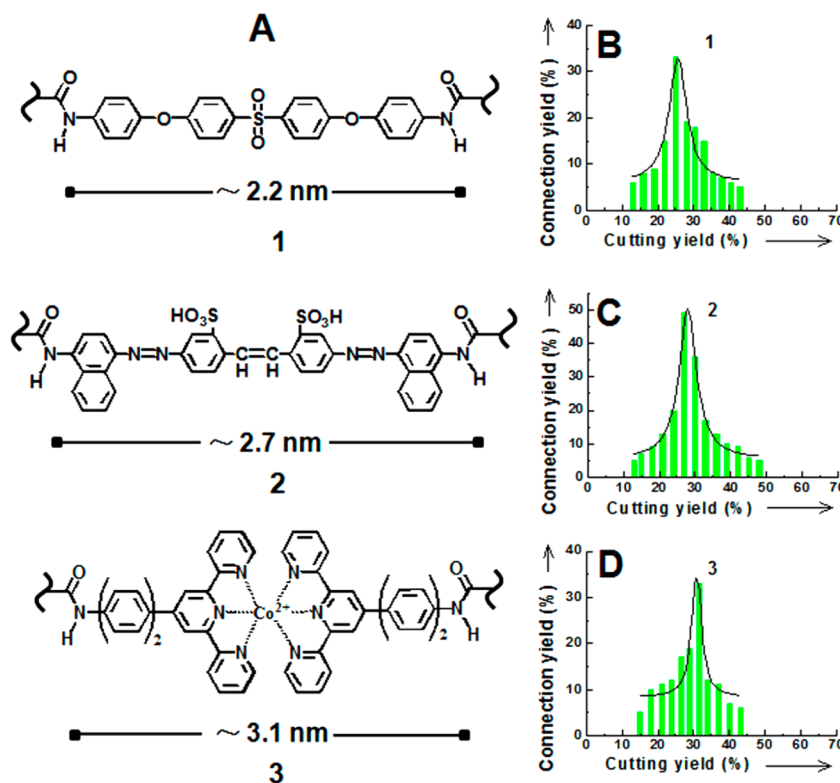

Figure 7. (A) Molecular structures of **1**−**3** used to reconnect graphene point contacts. Statistical data for the connection yields as a function of the cutting yields for (B) **1**, (C) **2**, and (D) **3**. The cutting yield is defined as the fraction of graphene FETs on a chip that are electrically disconnected after oxygen plasma etching; the connection yield is defined as the fraction of the completely broken devices that get reconnected after molecular connection.

allowed us to selectively and reversibly detect a single specific target molecule, thrombin, in real time.[38]

The aptamer used here was a 15-nucleotide single-stranded DNA with thymine 7 linkers on both 3′ and 5′ termini. The G4 conformation of this aptamer could be stabilized by K+ or Mg2+, and had a high binding affinity for thrombin (Figure 5B). The conductance of a representative device containing the aptamer exhibited a finite recovery when cut SWCNT electrodes were reconnected to the aptamer, primarily because of the formation of the native G4 conformation. However, after the device was immersed in thrombin buffer solution, its conductance increased by an order of magnitude (Figure 5C) from 8.5×10^{-5} to 8.6×10^{-4} e^2/h. We hypothesize that DNA-thrombin interactions rigidify the G4 conformation because the aptamer is highly flexible, unlike the usual distortion caused by proteins. The rigidified G4 conformation either has tighter π-stacking
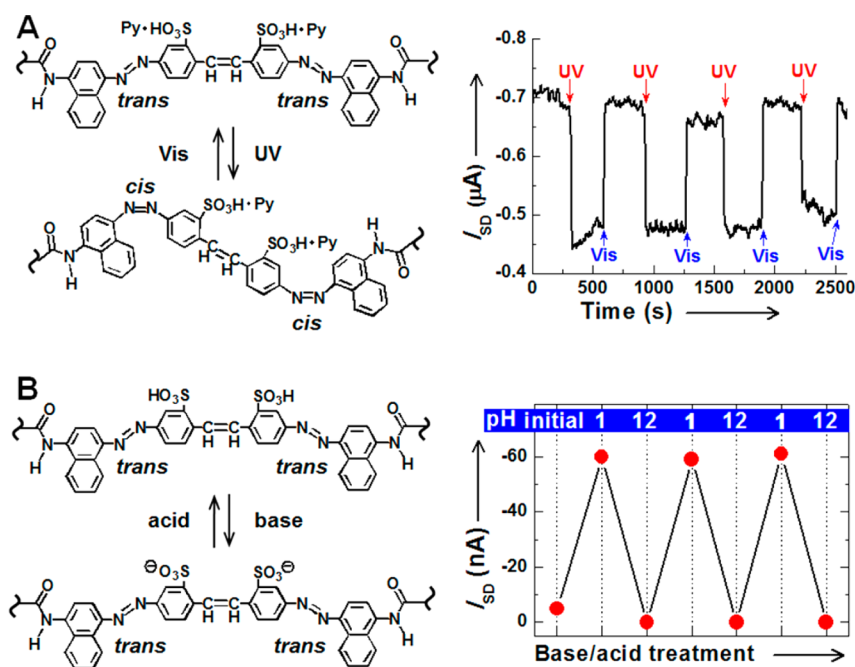
Figure 8. (A) Mechanistic demonstration and photoswitching properties of a graphene–azobenzene junction under irradiation with UV and visible lights. (B) Sensing mechanism and corresponding switching cycles by alternatively immersing the same device in solutions with low and high pH values (1 and 12, respectively).

along the charge transport path or provides an additional charge transport path via the central guanines, thus enhancing charge transport (Figure 5B).

To step toward real applications, we developed a practical method to fabricate high-density SWCNT transistor arrays. Figure 6A shows the integrated SWCNT transistor pattern used, where an individual SWCNT nicely spans all of the 80 metal electrodes. This method enabled us to achieve an average of one or two single-molecule junctions on each pattern. Because these molecular junctions have only one or at most two DNA probes available for protein accommodation, through combination with microfluidics (inset of Figure 6A), we realized real-time, label-free, reversible electrical detection of DNA–protein interactions with high selectivity, which reached real single-molecule sensitivity (Figure 6B). Compared with conventional optical techniques, this nanocircuit-based architecture is complementary but with obvious advantages such as no bleaching and no fluorescent labeling. This architecture offers a platform to explore the dynamics of stochastic processes in biological systems and gain information from genomics to proteomics to improve accurate molecular and even point-of-care clinical diagnosis.[39−41]

4.2. Graphene–Molecule Single-Molecule Junctions

4.2.1. Covalent Graphene–Molecule Junctions. To circumvent the challenges faced by SWCNT–molecule junctions of a relatively low yield of device fabrication and device variability, we developed another efficient lithographic method called dashed-line lithography to produce indented carboxylic acid-terminated graphene point contact arrays (Figure 1)[27] using high-quality large-area single-layer graphene universally available by chemical vapor deposition. To prove the effectiveness of this technique, we bridged these self-aligned point contacts with molecules capped by amino groups through amide formation in a pyridine solution containing the coupling agent 1-[3-(dimethylamino)propyl]-3-ethylcarbodiimide hydro-

chloride. Molecules **1**−**3** of different length shown in Figure 7A were used to construct graphene–molecule junctions. This method considerably simplified the device fabrication process and thus allowed us to optimize the fabrication conditions. Under optimized conditions, the general connection yield was about 30−50% or even higher, corresponding to about 28−33% of the graphene sheets that were completely cut (Figure 7B–D). On the basis of the binomial distribution calculation, if the connection yield is 20−30%, the ratio of single-junction devices to the overall reconnected devices is about 82−89%. This suggests that in most cases, only one or two junctions contribute to charge transport of each device.

4.2.2. Photon- or Proton-Gated Single-Molecule Sensors. The platform of graphene-molecule single-molecule junctions is robust and versatile because it has the flexibility to develop actual devices based on functional molecules that can transduce a variety of external physical stimuli. For example, a multifunctional molecule featuring azobenzene units and sulfonic acid groups (**2** in Figure 7A) was used to construct functional graphene–molecule junctions.[42] When the newly rejoined device was exposed to sequential irradiation with UV and visible lights, we observed cyclic changes of molecular conductance (Figure 8A). This observation was ascribed to the reversible conformational transformation of the azobenzene units of **2** between *trans* and *cis* isomers driven by light of different wavelengths. In another experiment, devices reconnected by **2** were detected under different pH conditions. We realized reproducible pH-gated conductance switching several times where the protonated states (pH = 1) were more conductive than the deprotonated ones (pH = 12) (Figure 8B). These results clearly demonstrate the possibility of integrating multiple functionalities into a single molecular device by rational molecular design, which invites further study.

4.2.3. Graphene–Diarylethene Single-Molecule Photoswitches. The ability to control the conductance of molecules at the molecular level by an external mode is still a
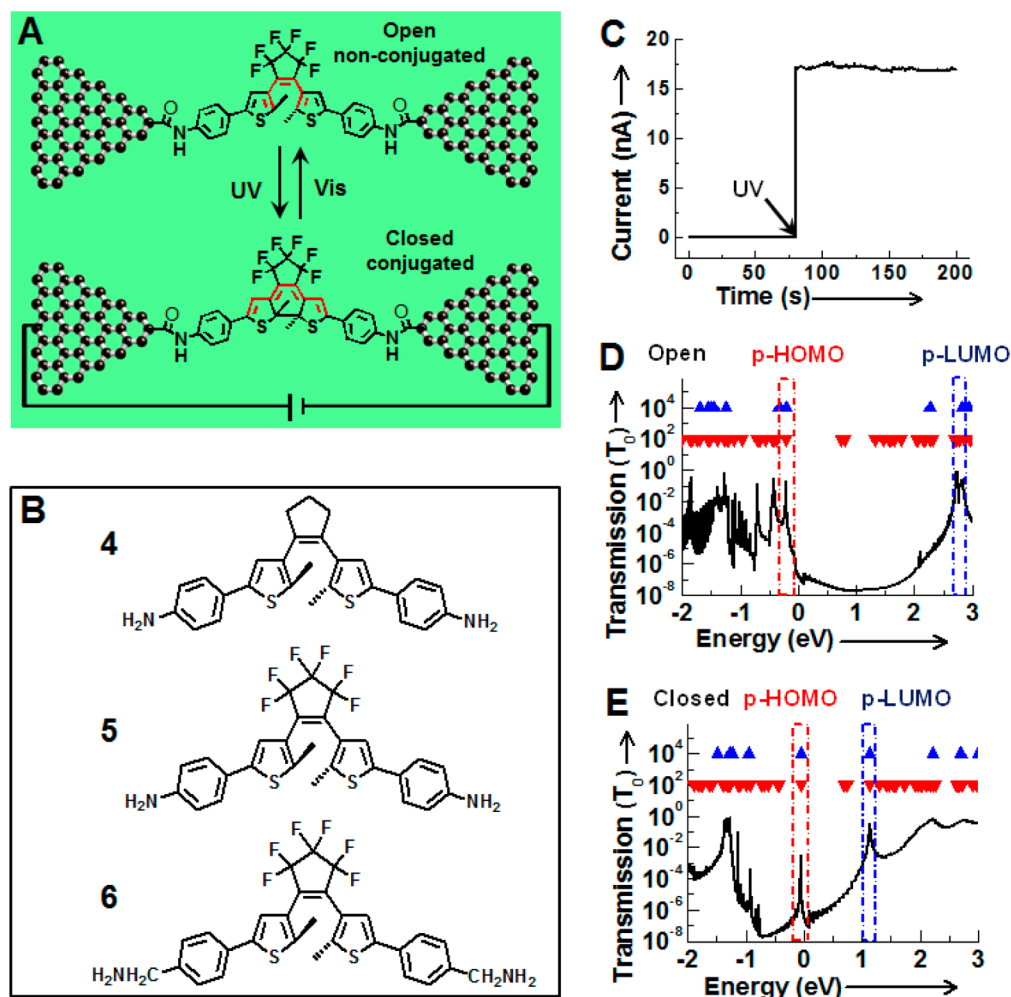
Figure 9. (A) Illustration of photoswitching in a graphene−DAE junction. (B) Molecular structures of **4**−**6**. (C) One-way photoswitching of a molecular junction containing **5** from off to on states under UV irradiation. (D, E) Zero-bias voltage transmission spectra of a junction containing **5** in (D) open and (E) closed forms.

formidable challenge in this field.[5,43,44] To construct single-molecule photoswitches, we wired diarylethene (DAE) molecules into nanogapped SWCNT electrodes.[43] Diarylethenes, as a typical family of photochromic molecules, can undergo reversible transitions between two distinct isomers with open and closed conformations when irradiated with light (Figure 9A). In addition to their superior thermal stability and fatigue resistance, these interesting electronic and structural properties make DAE molecules ideal candidates for building molecular photoswitches. However, because of the quenching induced by strong coupling between molecules and electrodes, only one-way photoswitching was observed. It remains a major challenge to conserve the favorable solution-based properties of molecules when immobilized in solid-state devices at the single-molecule level.[43,44]

Fortunately, the new platform of graphene−molecule single-molecule junctions simplifies device fabrication and thus provides the ability to tailor the alignment of energy levels at the molecule/electrode interface through molecular engineering.[45] Three DAE molecules, **4**−**6**, were rationally designed and synthesized. As shown in Figure 9B, **5** has a perfluorinated unit instead of the hydrogenated cyclopentene in **4**, while **6** has a methylene group (CH_2) between the terminal amine group and functional center on each side. Compared with **4**, **5** possesses

lower electron density on the central alkene unit because of the electron-withdrawing nature of the perfluorinated unit, and **6** has much weaker coupling with the electrodes because of the presence of saturated carbon atoms. Therefore, the energy levels of **5** are lower than those of **4**, while those of **6** are even lower. These molecular orbital calculations reveal that molecular engineering is a powerful way to modulate the electronic structure at the molecule/electrode interface, and consequently control the strong coupling between DAEs and electrodes.

Under low-intensity UV light (about 100 μW cm^{-2}, 365 nm) irradiation, all of the devices connected by any of the DAE molecules showed reproducible, substantial photoswitching from the low-conductance (off) state to the high-conductance (on) state (Figure 9C). We attribute this change in conductance to the photoinduced ring closure of the DAE providing a conjugated pathway between the two graphene electrodes in each device. The on/off ratios were very high, about 2 orders of magnitude. To better understand this phenomenon, we calculated the energy dependence of the transmission spectra of the devices (Figure 9D and E). The spectral features of the open and closed conformations are distinctively different near the Fermi level. In the closed state, the DAEs possess delocalized frontier orbitals with good
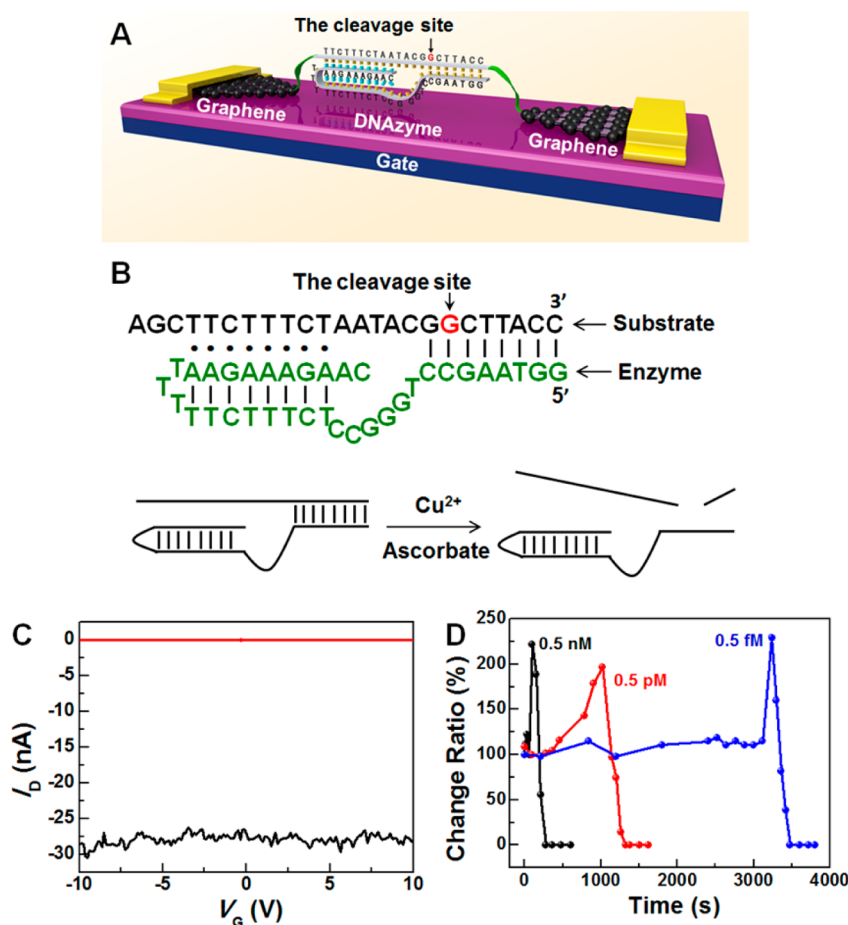
Figure 10. (A) Schematic representation of a graphene−DNAzyme junction. (B) Structural illustration of the Cu^{2+}-sensitive DNAzyme and corresponding catalytic process. (C) Device characteristics after DNAzyme connection (black) and further Cu^{2+} treatments (0.5 nM) for 5 min (red). (D) Concentration-dependent dynamics of the Cu^{2+} catalytic cleavage reactions.

conductive channels and have two strong transmission peaks located on each side of the Fermi level (about −0.05 and 1.2 eV; Figure 9E). These results readily explain why the closed state has higher conductance than the open state.

Regretfully, the coupling between **4**−**6** molecules and the electrodes was not weak enough to allow the working devices to revert back to the low-conductance state. To realize such reversibility, an obvious strategy would be to better control the interfacial coupling by rationally engineering the molecular backbone of DAEs.

4.2.4. Graphene−DNA Single-Molecule Biosensors. We also adapted the device architecture to achieve label-free metal ion detection, using Cu^{2+} as a representative, with femtomolar sensitivity and high selectivity by integrating a DNAzyme, which can catalytically cleave a DNA substrate at a specific site in the presence of Cu^{2+}, into graphene−molecule junctions (Figure 10A).[46] Figure 10A and B shows a DNA substrate with amino groups at both ends covalently sandwiched between carboxylic acid-capped graphene point contacts. The 5′ end of the DNAzyme binds to the substrate via Watson−Crick base pairs and the 3′ region through formation of a DNA triplex. The electrical characteristics of a representative device exhibited the finite conductance of the binding state (Figure 10C, black curve). After treatment with Cu^{2+}, the conductance decreased to zero (red curve in Figure 10C). This marked change should be attributed to the Cu^{2+}-assisted catalytic cleavage of the DNA substrate by the

DNAzyme resulting in a gap in the graphene−molecule junction (Figure 10B). To investigate the sensitivity of the graphene−DNA junction, different Cu^{2+} concentrations (0.5 nM, 0.5 pM, 0.05 pM, 5 fM, and 0.5 fM) were used to treat these newly reconnected devices. Figure 10D reveals that consistent conductance changes occurred in the presence of Cu^{2+}, even at concentrations as low as 0.5 fM, after a response time of about 60 min (Details can be found in ref 46). Because DNAzymes selective for a variety of metal ions can be obtained through in vitro selection, the sensing system demonstrated here can be applied to the detection of many other metal ions.

5. SUMMARY

Reliable and universal lithographic methodologies using a combination of ever-reducing top-down device fabrication with programmable bottom-up molecular assembly have been developed and successfully used to fabricate two classes of molecular electronic devices based on either SWCNTs or graphene as point contacts, thus opening a new direction in molecular electronics. The simplified device fabrication, promising device stability, and the ability to construct truly robust single-molecule devices offer unlimited opportunities to reveal and understand structure−function relationships at the molecular level, and then provide new design insights to developing novel types of molecular devices. Starting with the development of proof-of-principle strategies through to the application of molecular devices with desired functions, we have

not only examined the use of SWCNTs and graphene as efficient electrodes to build stimuli-responsive organic transistors at the macroscopic level, but also demonstrated the capability to install molecular functions in electrical circuits at the molecular level. As a result, we produced various functional devices that can operate as ion, pH, and light sensors and/or realize label-free, real-time electrical detection of biological interactions at the single-event level. These solid advances exemplify the remarkably fertile platform of carbon electrode—molecule junctions to study fundamental physical phenomena in the future, such as the quantum transport properties at low temperatures, thermoelectronics, optoelectronics, and single-molecule chemical and biological dynamics. In addition, the realization of atomic-level precision in the cutting procedure, and precise control of the molecular conformation on the substrate within the gaps and the contact configuration are challenges for future studies to overcome, of crucial importance to the development of this field from the laboratory-based research to practical applications.

AUTHOR INFORMATION

Corresponding Author
*E-mail: guoxf@pku.edu.cn.

Author Contributions
§C.J. and B.M. contributed equally to the work.

Notes
The authors declare no competing financial interest.

Biographies

Chuancheng Jia is currently a postdoctoral researcher in the College of Chemistry and Molecular Engineering, Peking University and Institute of Chemistry, Chinese Academy of Sciences, with Xuefeng Guo and Daoben Zhu. He received his Ph.D. degree in 2014 from the College of Chemistry and Molecular Engineering, Peking University, with Xuefeng Guo. His research is focused on single-molecule devices and dynamics.

Bangjun Ma is currently a Ph.D. candidate in the College of Chemistry and Molecular Engineering, Peking University, with Xuefeng Guo. He received his B.S. degree in 2012 from the College of Chemistry, Beijing Normal University. His research is focused on the development of the new-generation single-molecule junctions.

Na Xin is currently a PhD candidate in the College of Chemistry and Molecular Engineering, Peking University, with Xuefeng Guo. She received her B.S. degree in 2013 from the College of Chemistry and Chemical Engineering, Central South University. Her research is focused on device physics of single-molecule junctions.

Xuefeng Guo received his Ph.D. degree in 2004 from the Institute of Chemistry, Chinese Academy of Sciences, with Daoben Zhu and Deqing Zhang. From 2004 to 2007, he was a postdoctoral research scientist at the Columbia University Nanocenter with Colin Nuckolls and Philip Kim. He joined the faculty under "Peking 100-Talent" Program in 2008. In 2012, he won the National Science Funds for Distinguished Young Scholars in China. He has broad research interests, including nano/molecular electronics, organic/flexible electronics, and single-molecule detection/dynamics.

REFERENCES

(1) Kanjolia, R. K. New Materials in Semiconductor Fabrication: An Evolutionary Process. *Semicond. Int.* **2007**, *30*, 32−36.

(2) Wilson, L. *International Technology Roadmap for Semiconductors (ITRS)*; Semiconductor Industry Association: Washington, DC, 2013.

(3) Aviram, A.; Ratner, M. A. Molecular Rectifiers. *Chem. Phys. Lett.* **1974**, *29*, 277−283.

(4) Selzer, Y.; Allara, D. L. Single-Molecule Electrical Junctions. *Annu. Rev. Phys. Chem.* **2006**, *57*, 593−623.

(5) Jia, C.; Guo, X. Molecule-Electrode Interfaces in Molecular Electronic Devices. *Chem. Soc. Rev.* **2013**, *42*, 5642−5660.

(6) Aradhya, S. V.; Venkataraman, L. Single-Molecule Junctions Beyond Electronic Transport. *Nat. Nanotechnol.* **2013**, *8*, 399−410.

(7) Ratner, M. A Brief History of Molecular Electronics. *Nat. Nanotechnol.* **2013**, *8*, 378−381.

(8) Lörtscher, E. Wiring Molecules into Circuits. *Nat. Nanotechnol.* **2013**, *8*, 381−384.

(9) Sun, L.; Diaz-Fernandez, Y. A.; Gschneidtner, T. A.; Westerlund, F.; Lara-Avila, S.; Moth-Poulsen, K. Single-Molecule Electronics: From Chemical Design to Functional Devices. *Chem. Soc. Rev.* **2014**, *43*, 7378−7411.

(10) Tour, J. M. Molecular Electronics. Synthesis and Testing of Components. *Acc. Chem. Res.* **2000**, *33*, 791−804.

(11) Feldman, A. K.; Steigerwald, M. L.; Guo, X.; Nuckolls, C. Molecular Electronic Devices Based on Single-Walled Carbon Nanotube Electrodes. *Acc. Chem. Res.* **2008**, *41*, 1731−1741.

(12) Song, H.; Reed, M. A.; Lee, T. Single Molecule Electronic Devices. *Adv. Mater.* **2011**, *23*, 1583−1608.

(13) Li, T.; Hu, W. P.; Zhu, D. B. Nanogap Electrodes. *Adv. Mater.* **2010**, *22*, 286−300.

(14) Lindsay, S. M.; Ratner, M. A. Molecular Transport Junctions: Clearing Mists. *Adv. Mater.* **2007**, *19*, 23−31.

(15) McCreery, R. L.; Bergren, A. J. Progress with Molecular Electronic Junctions: Meeting Experimental Challenges in Design and Fabrication. *Adv. Mater.* **2009**, *21*, 4303−4322.

(16) Cao, Y.; Steigerwald, M. L.; Nuckolls, C.; Guo, X. Current Trends in Shrinking the Channel Length of Organic Transistors Down to the Nanoscale. *Adv. Mater.* **2010**, *22*, 20−32.

(17) Tao, N. J. Electron Transport in Molecular Junctions. *Nat. Nanotechnol.* **2006**, *1*, 173−181.

(18) Heath, J. R. Molecular Electronics. *Annu. Rev. Mater. Res.* **2009**, *39*, 1−23.

(19) Ulgut, B.; Abruna, H. D. Electron Transfer Through Molecules and Assemblies at Electrode Surfaces. *Chem. Rev.* **2008**, *108*, 2721−2736.

(20) Flood, A. H.; Stoddart, J. F.; Steuerman, D. W.; Heath, J. R. Whence Molecular Electronics? *Science* **2004**, *306*, 2055−2056.

(21) Nitzan, A.; Ratner, M. A. Electron Transport in Molecular Wire Junctions. *Science* **2003**, *300*, 1384−1389.

(22) Metzger, R. M. Unimolecular Rectifiers and Proposed Unimolecular Amplifier. *Ann. N. Y. Acad. Sci.* **2003**, *1006*, 252−276.

(23) Reed, M. A.; Lee, T. *Molecular Nanoelectronics*; American Scientific Publishers: Valencia, CA, 2003.

(24) Cuevas, J. C.; Scheer, E. *Molecular Electronics: An Introduction to Theory and Experiment*; World Scientific: Singapore, 2010.

(25) Cuniberti, G.; Fagas, G.; Richter, K. *Introducing Molecular Electronics*; Springer: New York, 2010.

(26) Haick, H.; Cahen, D. Making Contact: Connecting Molecules Electrically to the Macroscopic World. *Prog. Surf. Sci.* **2008**, *83*, 217−261.

(27) Cao, Y.; Dong, S.; Liu, S.; He, L.; Gan, L.; Yu, X.; Steigerwald, M. L.; Wu, X.; Liu, Z.; Guo, X. Building High-Throughput Molecular Junctions Using Indented Graphene Point Contacts. *Angew. Chem., Int. Ed.* **2012**, *51*, 12228−12232.

(28) Geim, A. K.; Novoselov, K. S. The Rise of Graphene. *Nat. Mater.* **2007**, *6*, 183−191.

(29) Jia, C.; Jiang, J.; Gan, L.; Guo, X. Direct Optical Characterization of Graphene Growth and Domains on Growth Substrates. *Sci. Rep.* **2012**, *2*, 707.

(30) Jia, C.; Li, H.; Jiang, J.; Wang, J.; Chen, H.; Cao, D.; Stoddart, J. F.; Guo, X. Interface-Engineered Bistable [2]Rotaxane-Graphene Hybrids with Logic Capabilities. *Adv. Mater.* **2013**, *25*, 6752−6759.

(31) Liu, S.; Wei, Z.; Cao, Y.; Gan, L.; Wang, Z.; Xu, W.; Guo, X.; Zhu, D. Ultrasensitive Water-Processed Monolayer Photodetectors. *Chem. Sci.* **2011**, *2*, 796−802.

(32) Cao, Y.; Liu, S.; Shen, Q.; Yan, K.; Li, P. J.; Xu, J.; Yu, D. P.; Steigerwald, M. L.; Nuckolls, C.; Liu, Z. F.; Guo, X. High-Performance Photoresponsive Organic Nanotransistors with Single-Layer Graphenes as Two-Dimensional Electrodes. *Adv. Funct. Mater.* **2009**, *19*, 2743−2748.

(33) Cao, Y.; Wei, Z. M.; Liu, S.; Gan, L.; Guo, X.; Xu, W.; Steigerwald, M. L.; Liu, Z. F.; Zhu, D. B. High-Performance Langmuir-Blodgett Monolayer Transistors with High Responsivity. *Angew. Chem., Int. Ed.* **2010**, *49*, 6319−6323.

(34) Lin, Y.; Guo, X. Ultrahigh Photo-Gain Nanoscale Hybrid Photodetectors. *Small* **2015**, *11*, 2856−2861.

(35) Li, S. S. *Semiconductor physical electronics*; Springer Science & Business Media: New York, 2007.

(36) Tanaka, K.; Tengeiji, A.; Kato, T.; Toyama, N.; Shionoya, M. A Discrete Self-Assembled Metal Array in Artificial DNA. *Science* **2003**, *299*, 1212−1213.

(37) Liu, S.; Clever, G. H.; Takezawa, Y.; Kaneko, M.; Tanaka, K.; Guo, X.; Shionoya, M. Direct Conductance Measurement of Individual Metallo-DNA Duplexes within Single-Molecule Break Junctions. *Angew. Chem., Int. Ed.* **2011**, *50*, 8886−8890.

(38) Liu, S.; Zhang, X.; Luo, W.; Wang, Z.; Guo, X.; Steigerwald, M. L.; Fang, X. Single-Molecule Detection of Proteins Using Aptamer-Functionalized Molecular Electronic Devices. *Angew. Chem., Int. Ed.* **2011**, *50*, 2496−2502.

(39) Choi, Y.; Moody, I. S.; Sims, P. C.; Hunt, S. R.; Corso, B. L.; Perez, I.; Weiss, G. A.; Collins, P. G. Single-Molecule lysozyme Dynamics Monitored by an Electronic Circuit. *Science* **2012**, *335*, 319−324.

(40) Wang, H.; Muren, N. B.; Ordinario, D.; Gorodetsky, A. A.; Barton, J. K.; Nuckolls, C. Transducing Methyltransferase Activity into Electrical Signals in a Carbon Nanotube-DNA Device. *Chem. Sci.* **2012**, *3*, 62−65.

(41) Sorgenfrei, S.; Chiu, C. Y.; Gonzalez, R. L.; Yu, Y. J.; Kim, P.; Nuckolls, C.; Shepard, K. L. Label-Free Single-Molecule Detection of DNA-Hybridization Kinetics with a Carbon Nanotube Field-Effect Transistor. *Nat. Nanotechnol.* **2011**, *6*, 126−132.

(42) Cao, Y.; Dong, S.; Liu, S.; Liu, Z.; Guo, X. Toward Functional Molecular Devices Based on Graphene-Molecule Junctions. *Angew. Chem., Int. Ed.* **2013**, *52*, 3906−3910.

(43) Whalley, A. C.; Steigerwald, M. L.; Guo, X.; Nuckolls, C. Reversible Switching in Molecular Electronic Devices. *J. Am. Chem. Soc.* **2007**, *129*, 12590−12591.

(44) Kim, Y.; Hellmuth, T. J.; Sysoiev, D.; Pauly, F.; Pietsch, T.; Wolf, J.; Erbe, A.; Huhn, T.; Groth, U.; Steiner, U. E.; Scheer, E. Charge Transport Characteristics of Diarylethene Photoswitching Single-Molecule Junctions. *Nano Lett.* **2012**, *12*, 3736−3742.

(45) Jia, C.; Wang, J.; Yao, C.; Cao, Y.; Zhong, Y.; Liu, Z.; Guo, X. Conductance Switching and Mechanisms in Single-Molecule Junctions. *Angew. Chem., Int. Ed.* **2013**, *52*, 8666−8670.

(46) Gao, L.; Li, L.-L.; Wang, X.; Wu, P.; Cao, Y.; Liang, B.; Li, X.; Lin, Y.; Lu, Y.; Guo, X. Graphene-DNAzyme Junctions: A platform for Label-free Metal Ion Detection with Ultrahigh Sensitivity. *Chem. Sci.* **2015**, *6*, 2469−2473.